

## INTERPRETATION OF AEROMAGNETIC DATA OVER PARTS OF BIDA BASIN, NORTH CENTRAL, NIGERIA

ALKALI, A., SALAKO, K. A., ADETONA, A. A., ALHASSAN, D. U., & UDENSI, E. E.

Department of Physics,  
Federal University of Technology Minna, Nigeria

Email: [aisha.alkali@futminna.edu.ng](mailto:aisha.alkali@futminna.edu.ng)

Phone No: +234-803-570-3809

### Abstract

*Interpretation of Magnetic Signatures over parts of central Bida Basin, Nigeria was carried out to highlight linear structures and to suggest the viability of the basin for hydrocarbon potentials in the survey area. Aeromagnetic data over the study area bounded by latitudes  $8.50^{\circ}N$  to  $10.00^{\circ}N$  and longitudes  $5.00^{\circ}E$  to  $6.00^{\circ}E$  was interpreted with a view to study the magnetic trends and to estimate the sedimentary thickness within the study area. Trend characteristics of magnetic lineaments were analysed using First Vertical Derivative. Source Parameter Imaging was used to estimate the sedimentary thickness. The Lineaments from the First Vertical Derivative trends majorly in NE-SW direction. The occurrence of subsurface linear structures may be due to discontinuities caused by faulting of country rock and this is in conformity with the history of the formation of the Bida Basin. The result of Source Parameter Imaging shows that depth to magnetic sources has its maximum sedimentary thickness of about 3.0 km in the south and central part of the study area. The sedimentary thickness of about 3.0 km might be sufficient for hydrocarbon maturation in the area.*

**Keywords:** *Basement, Lineaments, Magnetic Trend, Source Parameter Imaging, First Vertical Derivative*

### Introduction

The interpretation of aeromagnetic maps involves interpreting the basement structures and detailed examination of structures. The digitization method adopted for the study was the manual visual interpolation method. The aim of a magnetic survey is to investigate subsurface geology on the basis of anomalies in the earth's magnetic field resulting from the magnetic properties of the underlying rocks. Therefore, the aim is to determine the thickness of Bida Basement. Magnetic prospecting thus involves the measurement of variations in the earth's magnetic field. It is natural source methods in which local variations introduced by magnetic properties of rock near the surface causes minute changes in the main field. Determination of the structure and nature of the magnetized material is therefore an inverse problem of potential field theory. That is, the source is determined from its potential (Grant & West, 1965).

### Geology of the Area

The study area is located within the Bida Basin (also known as the Middle Niger Basin or the Nupe Basin) in the west - central part of Nigeria. The study areas cover Fashe, Akerre, Mokwa, Egbako, Lafiagi and Pategi. All the rocks in the study area belong either to the Upper Cretaceous or to the Precambrian. The sandstones of the Bida Basin belong to the Upper Cretaceous and they are underlain by the Precambrian rocks of the Basement Complex. (Russ, 1957; Adeleye, 1973 & 1976; Udensi *et al*, 2003). The Nupe sandstones consist of slightly cemented fine to coarse-grained sandstones and siltstones with interbedded thin beds of carbonaceous shales and clays. The Nupe sandstone appears to lie directly on the Basement (Adeleye, 1976). Figure 1 (Map of Nigeria) shows the location of the Study Area and Figure 2 is the geological map of the area. It lies between latitude  $8.50^{\circ}N$  and  $10.00^{\circ}N$  and longitude  $5.00^{\circ}E$  and  $6.00^{\circ}E$ .

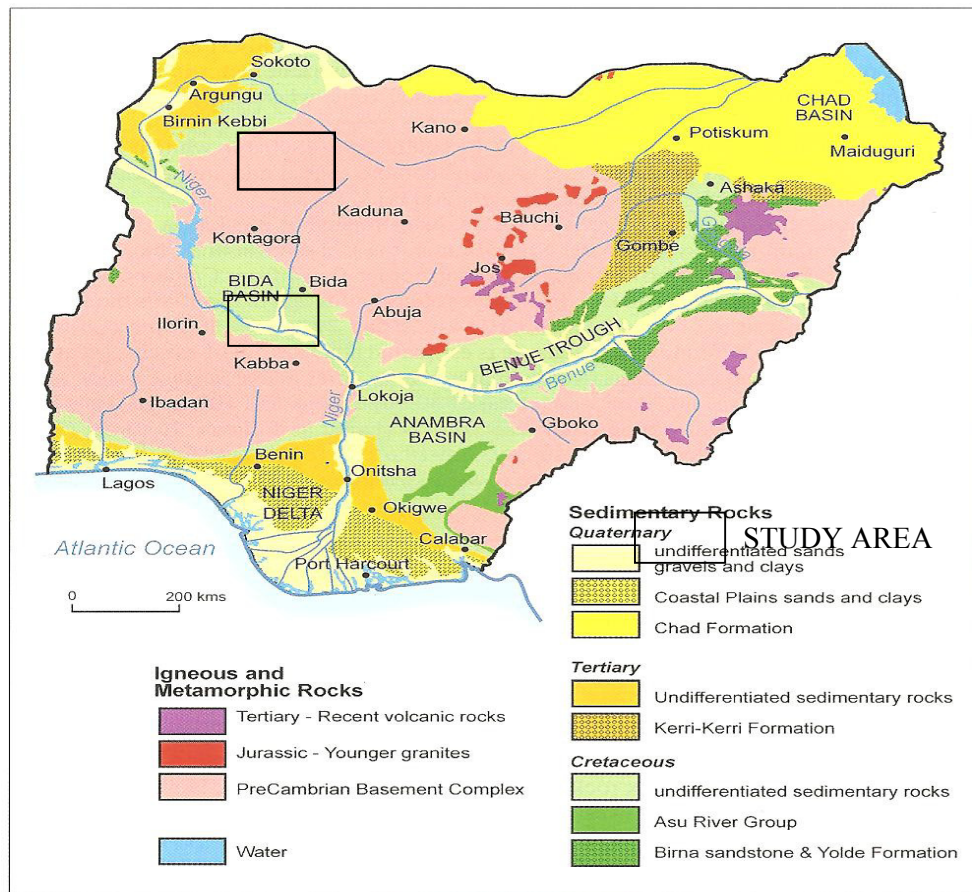


**Figure 1: Generalized Geological Map of Nigeria (Olasehinde & Amadi, 2009)**

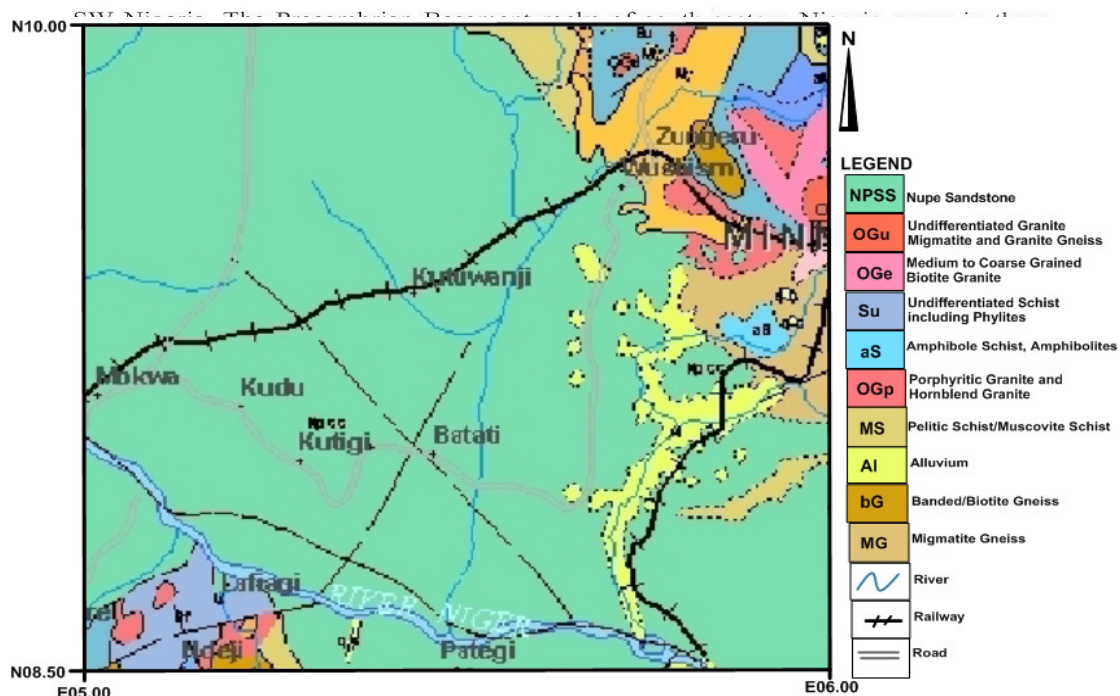


**Figure 2: Geological Map of the Study Area (Adapted from Nigeria Geological Survey Agency, 2006)**

## **Materials and Method**

### **Materials**

Data acquisition and analysis: Airborne magnetic survey of a substantial part of Nigeria was carried out by the Nigerian Geological Survey Agency between 1974 and 1980. The magnetic information consists of profiles or repetition flight lines plotted on continuous strip chart or tape records. To achieve this, the Nigerian landmass was divided into blocks. The magnetic data were collected at a nominal flight altitude of 500 ft (152.4m) along north-south flight lines spaced approximately 2 km apart. The data were published in the form of  $\frac{1}{2}$  degree by  $\frac{1}{2}$  degree aeromagnetic maps on a scale of 1:100, 000. The magnetic values were plotted at 10 nT intervals. The maps were numbered and names of the places of each map covers were written on them for easy reference. A total of 340 maps cover the entire country. The aeromagnetic maps covering the study area have been acquired from the Nigeria Geological Survey Agency. The study area is covered by aeromagnetic maps of sheet number 161,162,181,182, 203, and 204. The actual magnetic values within this block were reduced by 25,000 nT before plotting the contour maps. This means that a value of 25,000 nT was added to the contour values so as to obtain the actual field at a given point.

A correction based on the International Geomagnetic Reference Field (IGRF) epoch date January 1, 1974 was included in all the aeromagnetic maps published by the Nigerian Geological Survey Agency.

### **Aeromagnetic Map Digitization**

The Magnetic data for this research was acquired from the aeromagnetic maps covering part of the Bida Basin. The digitization method adopted for this study was the manual visual interpolation method. The visual interpolation method involves drawing of straight lines vertically and horizontally at equal spacing on a tracing paper to form a grid layout. The boundaries of the layout must coincide with the boundaries of the aeromagnetic map layout to be used for digitization (Udensi *et al.*, 2000). The layout is overlain on the aeromagnetic map and magnetic values were read at the junctions or cross points on the grid system. At grid points where the contour lines do not cross, visual interpolation to the closest contour line is made so as to estimate the magnetic value at the grid point. Since the grid points are evenly spaced, it is easy to determine the longitude and latitude of each grid point. The grid layout may be rectangular or square depending on the wish of the interpreter or the nature of the area concerned.

### **Production of Dataset (Super Data)**

The data from each digitized map is stored in a 37 by 57 coding sheet. Each sheet contains records of the boundary longitude and latitude, the map number and name of the town. The problem of boundary (edge) has to be solved before the combined dataset is produced. This problem is illustrated in (Figure 2), which represents a rectangular outline of the study area, Lafiagi, Pategi, Mokwa, Egbako, Fashe and Akerre sheets. Each small map is represented by the map number and contains 19 by 19 digitized magnetic values. At the boundary of two maps for example, maps (161) and (162), the field values in the last column of map (161) have the same coordinates (latitude and longitude) as the field values at the first column of map (162). Also at the boundary between map (161) and (182) the field values at the last row of map (161) have the same coordinates as the field values in the first row of map (182).

To have a dataset therefore, all magnetic values with the same coordinate must be added and averaged. So with this, the rows and columns of magnetic points with the same coordinate will not exist. Two ways through which this task could be achieved are:

- (i) A computer program can be designed to achieved the aim where one is dealing with large numbers of maps say from ten upwards.
- (ii) Use of manual manipulation when dealing with maps below ten, and care must be taken not to run into unnecessary errors.

When the last column and first column of the adjoining map is averaged, the new data value generated is recorded in place of the initial data value; the same process is repeated for the rows between two maps. At the end of this process, a set of data that is 37 by 37 grid was obtained. This gives a total of 1369 data points in the super map. Therefore, manual manipulation process was used for collection of data.

### **Production of the Unified Aeromagnetic Map (Super Map) of the Study Area**

The dataset (super data) cannot yet be contoured because the coordinates (latitude and longitude) of each of the data points are yet to be supplied. This was achieved using another Program like the one used for the small maps, which reads the data points row by row, and calculate their latitudes and longitudes using base values already supplied. The output is then in the form of columns of x, y, z where x, y and z represent longitude, latitude and the magnetic value of the given data point respectively. The output file from this program is subsequently fed into the SURFER- package for the production of the unified aeromagnetic map.

Magnetic data observed in geophysical surveys are the sum of magnetic fields produced by all underground sources. The terms "residual" and "regional" are used to differentiate between anomalies from local, near surface masses and those arising from larger and deeper features, respectively. The target for specific investigations are often small-scale structures buried at shallow depths, and the magnetic response of these targets are embedded in a regional field that arises from magnetic sources that are larger or deeper than the target or are located farther away. Correct estimation and removal of the regional field from the initial field observation yields the residual field produced by the target sources. Interpretation and numerical modelling are carried out on the residual field data; and the reliability of the interpretation depends to a great extend upon the success of the regional-residual separation, (Li & Oldenburg, 1998).

### **Methods**

#### **Vertical derivative**

A derivative tends to sharpen the edges of anomalies and enhance shallow features. The vertical derivative map is much more responsive to local influence than to broad or regional effect and therefore tends to give sharper picture than the map of the total field. Vertical derivative operator in the frequency domain is given by

$$L(r) = r^n \quad (1)$$

Where n is the order of differentiation, and r is the wavenumber (radians/ground unit) The vertical derivative is commonly applied to total magnetic field data to enhance the shallowest geologic sources in the data. As with other filters that enhance the high-wavenumber components of the spectrum, you must often also apply low-pass filters to remove high-wave number noise. This is a measure of the curvature of the field. The second vertical derivative enhances geologic feature which generate greater curvature of the magnetic field. This is the case for anomalies from geologic features that are close to the surface. In addition to enhancing weaker anomalies, the second vertical derivative can often be used to delineate the contacts of lithologies with contrasting physical properties such as densities, and susceptibilities, (Bhattacharyya, 1966; Henderson & Zietz, 1967).

### Source Parameter Imaging (SPI)

Source Parameter Imaging (SPI) function is a quick, easy, and powerful method for calculating the depth of magnetic sources. Its accuracy has been shown to be +/- 20% in tests on real data sets with drill hole control. This accuracy is similar to that of Euler deconvolution, however SPI has the advantage of producing a more complete set of coherent solution points and it is easier to use.

A stated goal of the SPI method (Thurston and Smith, 1997) is that the resulting images can be easily interpreted by someone who is an expert in the local geology. The SPI method (Thurston and Smith, 1997) estimates the depth from the local wave number of the analytical signal. The analytical signal  $A_1(x, z)$  is defined by Nabighian (1972) as:

$$A_1(x, z) = i \frac{\partial M(x, z)}{\partial x} - j \frac{\partial M(x, z)}{\partial z} \quad (2)$$

Where  $M(x, z)$  is the magnitude of the anomalous total magnetic field,  $j$  is the imaginary number,  $z$  and  $x$  are Cartesian coordinates for the vertical direction and the horizontal direction respectively. From the work of Nabighian (1972), he shows that the horizontal and vertical derivatives comprising the real and imaginary parts of the 2D analytical signal are related as follows:

$$\frac{\partial M(x, z)}{\partial x} \Leftrightarrow - \frac{\partial M(x, z)}{\partial z} \quad (3)$$

Where  $\Leftrightarrow$  denotes a Hilbert transformation pair. The local wave number  $k_1$  is defined by Thurston and Smith (1997) to be

$$k_1 = \frac{\partial}{\partial x} \tan^{-1} \left[ \frac{\frac{\partial M}{\partial z}}{\frac{\partial M}{\partial x}} \right] \quad (4)$$

The concept of an analytical signal comprising second-order derivatives of the total field, can be used in a manner similar to that used by Hsu *et al.* (1996). The Hilbert transform and the vertical-derivative operators are linear, so the vertical derivative of (3) will give the Hilbert transform pair,

$$\frac{\partial^2 M(x, z)}{\partial x \partial x} \Leftrightarrow - \frac{\partial^2 M(x, z)}{\partial^2 z} \quad (5)$$

Thus the analytical signal could be defined based on second-order derivatives,  $A_2(x, z)$ , where

$$A_2(x, z) = \frac{\partial^2 M(x, z)}{\partial x \partial x} - j \frac{\partial^2 M(x, z)}{\partial^2 z} \quad (6)$$

This gives rise to a second-order local wave number  $k_2$ , where

$$k_2 = \frac{\partial}{\partial x} \tan^{-1} \left[ \frac{\frac{\partial^2 M}{\partial^2 z}}{\frac{\partial^2 M}{\partial x \partial x}} \right] \quad (7)$$

The first- and second-order local wave numbers are used to determine the most appropriate model and depth estimate independent of any assumptions about a model.

Nabighian (1972) gives the expression for the vertical and horizontal gradient of a sloping contact model as:



$$\frac{\partial M}{\partial x} = 2KFc \sin d \frac{h_c \cos(2I-d-90) + x \sin(2I-d-90)}{h_c^2 + x^2} \quad (8)$$

$$\frac{\partial M}{\partial z} = 2KFc \sin d \frac{x \cos(2I-d-90) + h_c \sin(2I-d-90)}{h_c^2 + x^2} \quad (9)$$

Where  $K$  is the susceptibility contrast at the contact,  $F$  is the magnitude of the earth's magnetic field (the inducing field),  $c = 1 - \cos^2 i \sin^2 \alpha$ ,  $\alpha$  is the angle between the positive x-axis and magnetic north,  $i$  is the ambient-field inclination,  $\tan I = \sin i / \cos \alpha$ ,  $d$  is the dip (measured from the positive x-axis),  $h_c$  is the depth to the top of the contact and all trigonometric arguments are in degrees. The coordinate system has been defined such that the origin of the profile line ( $x = 0$ ) is directly over the edge.

The expression for the magnetic-field anomaly due to a dipping thin sheet is

$$M(x, z) = 2KFwS \frac{h_1 \sin(2I-d) - x \cos(2I-d)}{h_1^2 + x^2} \quad (10)$$

where  $w$  is the thickness and  $h_1$  the depth to the top of the thin sheet. The expression for the magnetic-field anomaly due to a long horizontal cylinder according to Nabighian, M.N. (1984) is

$$M(x, z) = 2KFS \frac{\sin i (h_h^2 - x^2) \cos(2I-180) + 2xh_h \sin(2I-180)}{(h_h^2 + x^2)^2} \quad (11)$$

$S$  is the cross-sectional area and  $h_h$  is the depth to the centre of the horizontal cylinder. Substituting (8), (9), (10) and (11) into the expression for the first- and second-order local wave number ( $K_1$  &  $K_2$ ) After some simplification yield a remarkable result (12) and (13) as were obtained.

$$K_1 = \frac{(n_k + 1)h_k}{h_k^2 + x^2} \quad (12)$$

and

$$K_2 = \frac{(n_k + 1)h_k}{h_k^2 + x^2} \quad (13)$$

Where  $n_k$  is the SPI structural index (subscript  $k = c, t$  or  $h$ ), and  $n_c = 0$ ,  $n_t = 1$  and  $n_h = 2$  for the contact, thin sheet and horizontal cylinder models, respectively.

From (12) and (13) above, it is evident that the first- and second-order local wave numbers are independent of the susceptibility contrast, the dip of the source and the inclination, declination, and the strength of the earth's magnetic field.

## Results and Discussion

### Qualitative trend analysis

Figure 3 is the total magnetic intensity map of the study area. It shows a colour range of total magnetic intensity anomalies of high and low magnetic intensity values which dominate northeast-southwest trends. The blank area in the map shows plain or missing data, the total magnetic intensity anomaly highs are dominant in the north-eastern, south-eastern and west-central part of the Bida Basin, while total magnetic intensity anomaly lows are dominant in the north, central and southern portions of the study area. Since sedimentary rocks have low susceptibility values, the observed magnetic high anomaly closures within the basin area may originate from the underlying basement rocks beneath the basin or from intrusive rocks which might have intruded into the basin section (Udensi et al., 2000). The resultant TMI map in Figure 3 comprises of high, low and intermediate magnetic signatures which could be attributed to (a) rock susceptibility (b) depth to the source magnetic rock (c) degree of strike and (d) remnant magnetization (Sunday, 2012).

Trend and lineation are the major information of qualitative analysis which are usually an indication of the features that give rise to faults and fractures (Udensi et al., 2003). In the study area, (Figure 3) shows a colour range of total magnetic intensity values, with pink as high and blue as low. The dominant trends is Northeast-Southwest trends and are observed around Mokwa area in the Northwest portion and around Pategi in the Southeast portion. Also, northeast-southwest trend is observed around Lafiagi in the central portion of the area. Several magnetic high and low dot the study area and are usually paired together. The high are concentrated on the Southeast direction while the low are concentrated on the northwest direction. It also shows that the area is composed of different magnetic region that are differentiated on the basis of variation of intensities of magnetic response. The North western part of the study area is characterized by high magnetic response, trending Northeast-Southwest. The North-Eastern part of the map is also characterized by high magnetic anomalies and lows magnetic anomalies trending East-west direction. Finally, the central part of the map represented by the blue colour is characterized by low magnetic response trending Eastwest and Northeast-Southwest direction represent Pan African trend. This is in accordance of the work carried out by (Buser, 1966). He established the existence of Paleostructures which were due to tectonic movements, intrusion, metamorphism, sedimentation, mineralization, volcanism and drainage.

### **First Vertical Derivative**

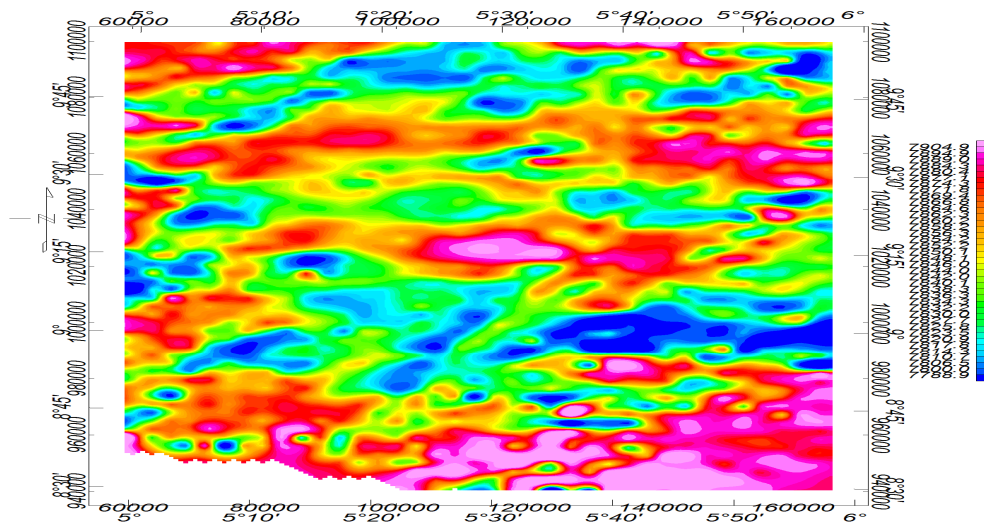
Figure 4 shows the lineament derived from the first vertical derivative map. Several lineaments were labelled from F1-F17. The southern part of the map is remarkably characterized by high distortion in the magnetic signatures which are signatures of basement regions. The central part is characterized by long wavelength anomalies which represent the sedimentary region. These lineaments have been interpreted as combinations of lithologic contacts, basement fault line. Most of the fault line and fractures identified within the study area are trending NE-SW and this is in conformity with the history of the formation of the Bida Basin (Udensi et al., 2003).

### **Correlation of First Vertical Derivative Map and Lineament Map**

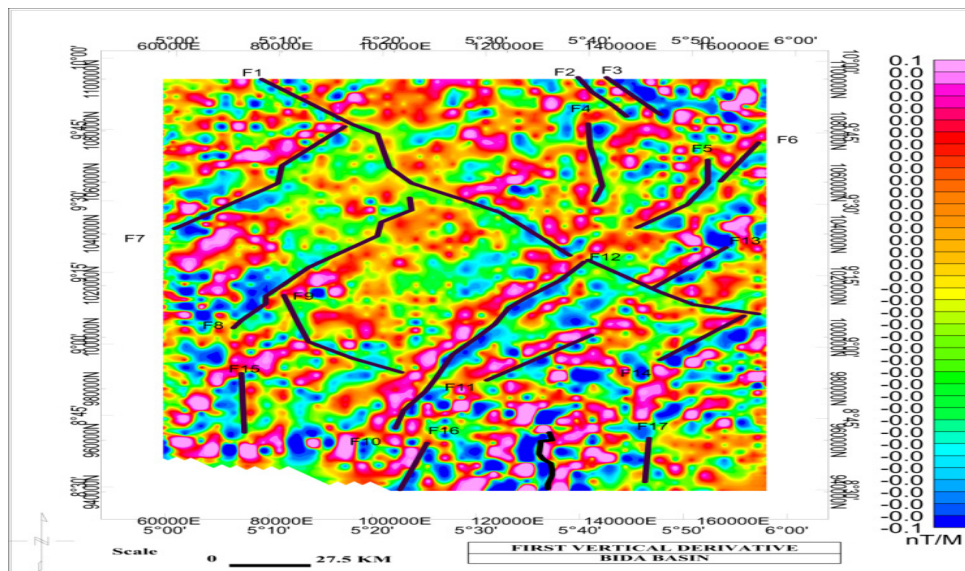
Figure 5 shows the correlation of first vertical derivative map and lineament maps on the basis of lineaments. The prominent trend directions common to both maps are the northeast-southwest and northwest-southeast directions. This is in agreement with Udensi *et al.*, (2003) and Ajakaiye *et al.*, (1991).

### **Source Parameter Imaging (SPI)**

The result of the Source Parameter Imaging analysis of the aeromagnetic data over part of Bida Basin identified two main magnetic horizons under the area; the deeper sources are represented by the low frequency components while shallower magnetic sources are represented by the high frequency components (Figure 6a). The maximum thickness of sediment found in the study area is about 3.0 km. These areas are targets for hydrocarbon accumulation in the Bida Basin.



**Figure 3: Total Magnetic Intensity Map of the Study Area after 25,000nT have Been Removed**





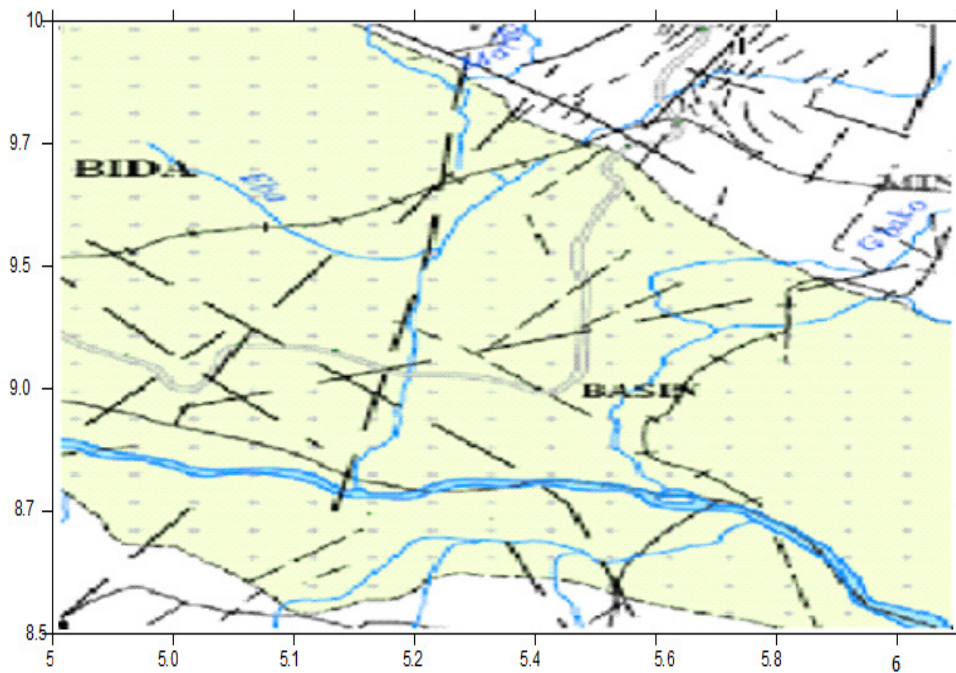
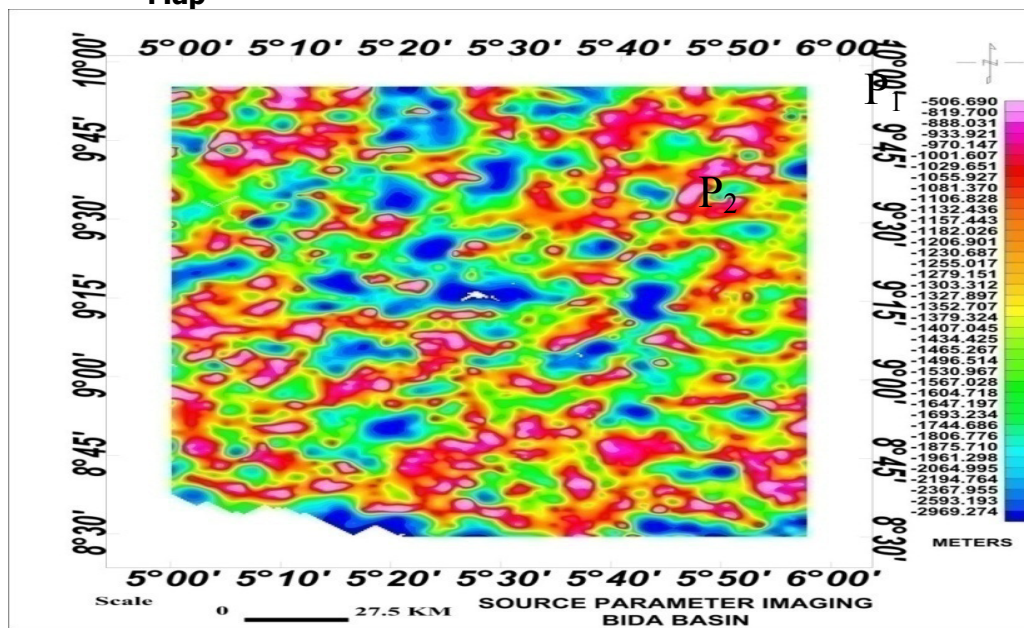
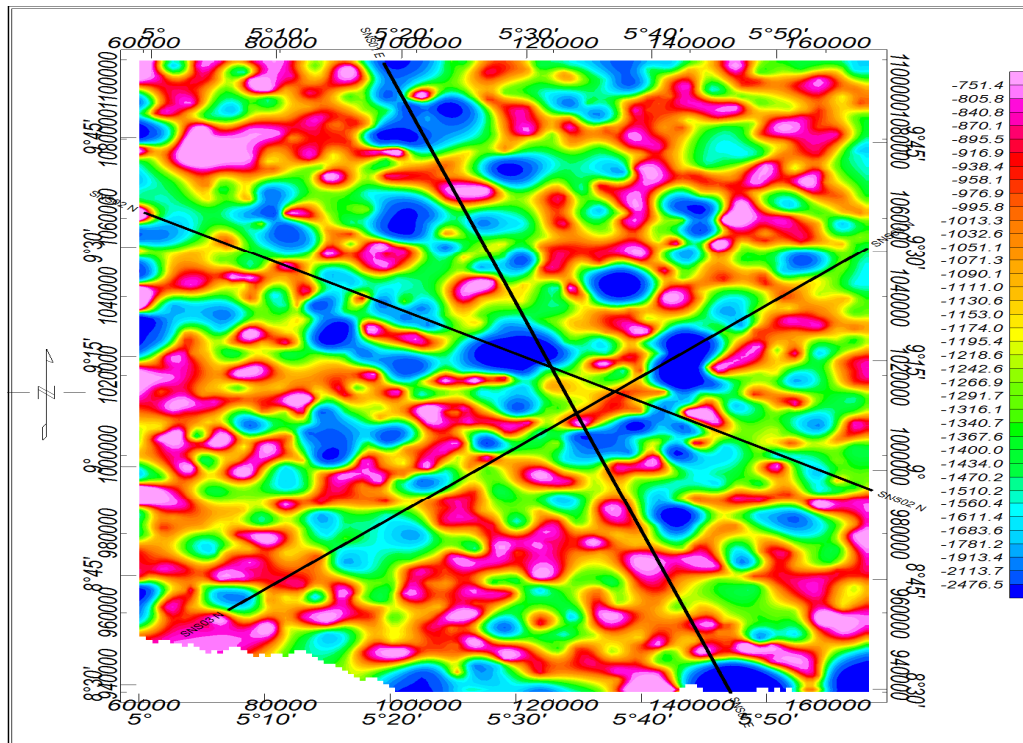


Figure 4: First Vertical Derivative Map of the study area. Figure 5: Lineament Map



$P_3$



**Figure 6(a): Source Parameter Imaging of the Study Area (b) SPI with Three Profile Lines**

Three profiles were drawn across SPI Map, Figure 6b. These profiles were carefully drawn such that the areas of considerable sedimentary thicknesses were covered. Profile 1 (Figure 7a) was drawn in the direction of NNW-SSE. The profile has its highest sedimentary thickness of about 3.8 km at the edge of the profile. Profile 2 (Figure 7b) was drawn in the direction of NW-SE. The profile has its highest sedimentary thickness of about 4.0 km at the central portion of the profile. Profile 3 (Figure 7c) was drawn in the direction of SW-NE. The profile has its highest sedimentary thickness of about 3.5 km at edge of the profile. Profile 2 (Figure 7b) has the highest sedimentary thickness along Mokwa area in the NW portion and around pategi in the SE part of the study area.

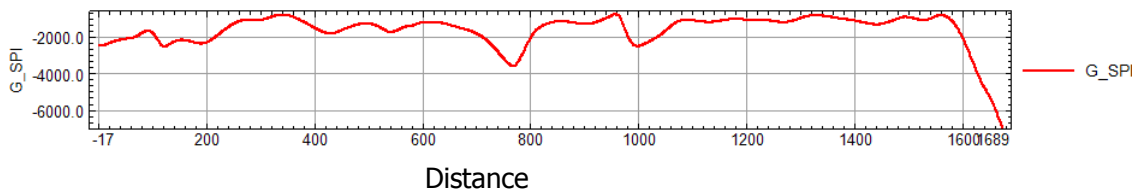


**Figure 7a: Profile 1 drawn in NNW-SSE direction in Figure 6b**

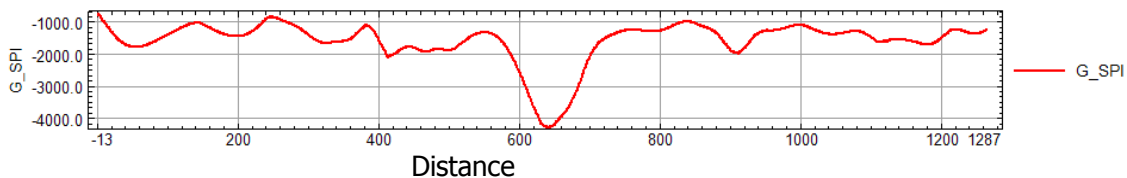


**Figure 7b: Profile 2 drawn in NW-SE direction in Figure 6b**

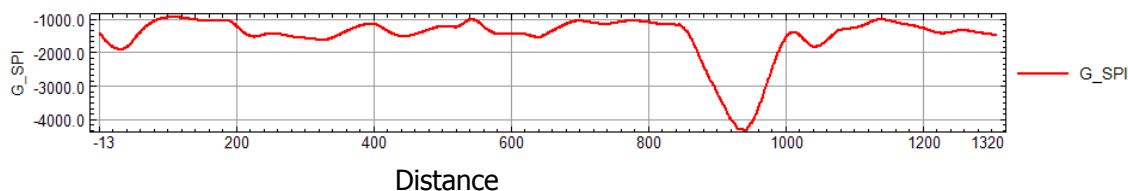


**Figure 7c: Profile 3 drawn in SW-NE direction in Figure 6b**

### Conclusion

Investigation of Magnetic Trends using aeromagnetic map was carried out in the central part of the Bida Basin using Vertical Derivative, and Source Parameter Imaging. Analysis of the Total Magnetic Intensity map shows a combination of both high and low magnetic closures due to variation in intensity values. The highs, lows and intermediate magnetic signatures could be attributed to: (a) rock susceptibility, (b) depth to the source magnetic rock, (c) degree of strike and (d) remanant magnetization. The total magnetic intensity (TMI) data was reduced to equator.

The Aeromagnetic Data was analysed using the First Vertical Derivative analysis which represent sedimentary region with several lineaments labelled as F1-F17. These lineaments have been interpreted as combinations of lithological contacts, and basement fault line. Most of the fault line and fractures identified within the study area are trending NE-SW and this is in conformity with the history of the formation of the Bida basin. The economic mineral present in the study area may be found along the lineaments delineated, since most magnetic minerals are structurally controlled.

The result of the Source Parameter Imaging analysis identified two main magnetic horizons under the area, the deeper sources are represented by the low frequency sources while shallower magnetic sources are represented by the high frequency sources and the thickness of sediment of about 3.0 km is found in the south and central part of the study area. These areas are targets for the hydrocarbon accumulation in the Bida Basin and therefore recommended for seismic survey and borehole logging for further investigation.

### References

- Adeleye, D. R. (1973). Origin of ironstones: An example from middle Niger valley. *Nigerian Journal of Sedimentary Petrology*, 43, 709 - 727.
- Adeleye, D. R. (1976). The geology of middle Niger basin. Lagos: *Geology of Nigeria*, Elizabethan. Pp. 283 - 287
- Ajakaiye, D. E., Hall, D. H., Ashiekaa, J. A., & Udensi, E. E. (1991). Magnetic anomalies in the Nigerian Continental mass based on aeromagnetic survey. *Tectonophysics*, 192, 211-230.
- Bhattacharyya, B. V. K. (1966). A method for computing the total magnetization vector and the dimensions of a rectangular block-shaped body from magnetic anomalies. *Geophysics*, 31, 74-96.
- Grant, F. S. & West, G. F. (1965). *Interpretation theory in Applied Geophysics*. New York: McGraw-Hill Book Co.

- Henderson, R. G. & Zietz, I. (1967). The computation of second vertical derivative of geomagnetic fields. *Mining Geophysics*, 2, 606 - 614.
- Hsu, S. K., Sibuet, J. C., & Shyu, C. T. (1996). High resolution detection of geologic boundaries from Potential Field Anomalies: An enhanced analytic signal technique. *Geophysics*, 61, 373 - 386.
- Li, Y., & Oldenburg, D. W. (1998). Separation of regional and residual magnetic field data. *Geophysics*, 63, 431 - 439.
- Nabighian, M. N. (1972). The analytical signal of two dimensional bodies with polygonal cross section: Its properties and use for automated anomaly interpretation. *Geophysics*, 37, 507 - 517.
- Nabighian, M. N. (1984). Toward a three-dimensional automatic interpretation of potential field data via generalized Hilbert transform: Fundamental relations. *Geophysics*, 47, 780 - 786.
- Russ, W. (1957). The Geology of part of Niger, Zaria and Sokoto Province. *Geological Survey of Nigeria Bulletin*, 27, 1 - 42.
- Salako, (2014). Depth to basement determination using source parameter imaging (SPI) of aeromagnetic data: An application to upper Benue trough and Borno basin, Northeast, Nigeria. *Academic Research International*, 5(3).
- Sunday, J. (2012). *Estimation of magnetic source depths from aeromagnetic data of Maiduguri source depths from aeromagnetic data of Maiduguri using gradient inversion*. M. Sc Thesis. Department of Physics, University of Ilorin.
- Thurston, J. B., & Smith, R. S. (1997). Automatic conversion of magnetic data to depth, dip, and susceptibility contrast using the SPI TM method. *Geophysics*, 62, 807- 813.
- Udensi, E. E, Osazuwa, I. B. & Daniyan, M. A. (2000). Production of a composite aeromagnetic map of the Nupe basin, Nigeria. *Nigerian Journal of Science, Technology and Mathematics Education*, 3(2),150-159.
- Udensi, E. E., Osazuwa, I. B., & Daniyan, M. A. (2003). Trend analysis of the total magnetic field over the Bida basin, Nigeria. *Nigerian Journal of Physics*, 15(1), 143-151.